Optimal Frequency Deviations Control in Microgrid Interconnected Systems

M.W. Siti[1], D.H. Tungadio[2], Y. Sun[2], N.T. Mbungu[3*], R. Tiako[4]

[1] Department of Electrical Engineering, Tshwane University of Technology, Pretoria, South Africa
[2]Department of Electrical and Electronic Engineering, University of Johannesburg, Johannesburg, South Africa
[3] Department of Electrical, Electronics and Computer Engineering, University of Pretoria, Pretoria, South Africa
[4] Department of Electrical Engineering, University of KwaZulu-Natal, Durban, South Africa
[*]mbungunsilulu@gmail.com

Abstract: The increase in the price of fossil fuel due to its rarity and emissions means more integration of renewable energy sources (RES) is required to improve economic management of the grid. This paper analyses a combination of the tie-line power between conventional power sources and the renewable energy system and its frequency deviations which are known as area control error. The minimisation of the tie-line by optimal control is effected in such a way that the frequency and tie-line power error can be minimised while maintaining the power balance between generation and load. The tie-line connected to the microgrid consists of two main parts, namely the conventional source and the renewable energy source, each made up of a synchronous generator. The control application of the active power and frequency to a network is referred to as load frequency control (LFC) with the storage system as an integral part of RES. The simulation results show the performance of the proposed optimal control model in microgrid during the changing loads' condition, where the energy storage system applied to optimal control has shown a quick response to frequency deviation, which is close to 80%.

1. Introduction

The electrical system is becoming increasingly complex in terms of energy demand and power quality, while energy saving is turning into an issue of concern. Several techniques regarding energy management and optimisation have been developed to ensure the quality of the electrical power system. This is often characterised by the interaction and coordination of various electrical sub-systems or areas, where each region is connected to the others by a tie-line [1]. Therefore, stabilising the electrical power system entails maintaining the power flow on the tie-line at its net value[2] [3]. On the other hand, managing the energy flow of a large scale microgrid which is not connected to any tie line can support the utility grid [4].

The integration of renewable energy into the electrical power system is often seen as a possible way of stabilising and ensuring power quality of the electrical grid [5][6]. As one of the cleanest and most suitable energy sources, renewable energy helps the electrical engineer to satisfy the energy demand of the power system in peak time. The most popular renewable energy resources are the wind turbine and photovoltaic systems [7][8]. Such methods are used in combination or separately in a standalone system or connected to the electrical grid [9]. The interconnection of the electrical network with renewable energy resources can affect the entire power system because of the random nature of wind and solar power [10]. Thus, a storage system is introduced to stabilise the power system during the low production of each renewable energy resource or all of them simultaneously[11]. The concept of a microgrid is introduced when the electrical load is supplied with a low voltage in using the storage system. This involves several energy resources, such as distributed sources (municipal supply) and distributed generators (wind, solar)[12][13]. The microgrid system is developed in medium voltage, and the rated power of a microgrid can be up to 10 MVA [14]. A microgrid can function as a standalone system or be connected to the utility grid [15]. When it is connected to the distributed sources, it is essential to control the frequency stability because of the random nature of renewable energy and the active control power to make it more flexible for load control analysis.

Recently, several research works developed an optimal control behaviour that can support load frequency regulation of microgrids by optimally integrating renewable energy resources and energy storage system. Additionally, the frequency is a significant quantity which must always be controlled to verify the dynamic of the energy balance and the generation. In [16], based on the main challenges associated with the wind energy integrated into the grid, an autonomous hybrid power is designed. The authors in [17] presented the power modulation of the PV generator for frequency control; the PV is used as a small electric double layer capacitor that absorbs rapid fluctuations and allows the generator to change its output at a limited rate. In [18], an optimal hybrid power system connected to the utility grid for industrial application is designed under model predictive control for reducing the overall operation cost. In [19], autonomous microgrids with demand response and renewable resources are evaluated to cover the uncertainties in renewable energy resources and electricity demand. The system is designed under the risk-neutral stochastic optimisation algorithm to maximise the expected profit of the system operator.

It is worth noting that with the integration of the microgrids into the electrical network, the system is becoming more complex and challenging to operate and needs a more flexible optimal operation and control. Thus, the Battery Energy Storage System (BESS) can provide fast and active power compensation. The authors in [11] discussed the benefit of BESS. It is observed that the BESS also improves the reliability of supply during the peak variation of the load in different interconnected areas. The energy storage facilities possess additional dynamic benefits

such as load levelling, factor correction and black start capability. Martinez et al. in [20] proposed an optimal sizing strategy of energy storage to ensure LFC in the electrical power system, which is connected to intermittent wind generation. The proposed model also evaluated the influence of energy storage on LFC through probabilistic tools to minimise the overall cost of the system.

In power system analysis there is a relationship between the active power and frequency. The control of frequency by the action between two or more areas is defined as LFC. The primary role of the approach in the power system is to keep the frequency constant against load variation and regulate the tie-line power exchange error. In most cases, when there is a variation in the load, the impact on a generating unit is seen as an imbalance between the real power input and output [21]. In [1], predictive active power control of two interconnected microgrids is proposed. The designed system applied a predictive regulator algorithm to control the energy flow in tie-lines and frequency deviations of the system, between the energy generation and the energy demand. In [22], LFC strategy such as conventional PID, expert systems like fuzzy logic and the neural network have been applied to overcome the pitfalls of a traditional controller.

In [23], hybridised fuzzy-conventional model structures are designed to deal with the impacts of the capacitive energy storage units. The system used the automatic generation control for an interconnected power system so that a dynamic performance of the electrical system can be created to optimise the energy flow. The proposed hybrid control is robust to handle the parameter uncertainty of the system in the presence of disturbances rejection. However, the system parameters are chosen based on specific empirical strategies which are not often recommended. In [24], frequency stabilisation under a sensitivity analysis is proposed. The model aims to avoid the system disturbance rejection by integrating superconducting magnetic energy storage and thyristor controlled series compensator into the interconnected power system. The system also used the strategy of automatic generation control to guarantee the dynamic stability of the different units on the network. In [25], the dynamic of battery storage is interconnected in a three area environment that contains thermal-gas-hydro-power system. There is satisfactory improvement of the system in terms of system performance and decrease in overshoots of dynamic frequency deviation under load disturbances. The design strategy exploits the automatic generation control in each area where the designed plant is developed through the Particle Swarm optimisation to coordinate the LFC of the system.

In [26], an artificial neural network application is designed to control the load frequency of a microgrid. The proposed neural network controller is compared to a conventional Proportional Integral (PI). The proposed neural controller improved the system regarding dynamic response for a step load change. In [27] the dynamic model of BESS is introduced for the LFC on an interconnected reheat thermal system. In [28] the BESS for LFC is proposed to improve the system. The design model used the dynamic strategy of the battery to deal with the power flow controller and system performance. The approach is more performant compared to the conventional control scheme used in LFC of the power system. It is observed that the BESS provided a satisfactory solution that comes with capability, feasibility and reliability, with accuracy in LFC of the interconnected power systems.

However, several breaches were found in the context of combining optimisation, planning and control and energy management for microgrid applications that can provide load frequency regulation. Therefore, the objective of this study is to minimise frequency when there is a load change between areas and to maintain the net tie-line power flow out of the area at its scheduled value. For each field to absorb its load changes, the use of the dynamic of the battery energy storage system as control has an advantage over the conventional control, such as the PID, PI and enhances the time response and the accuracy to control the energy flow. This is the main reason why an optimal control is proposed in this study. Optimal control model was traditionally conceived to solve continuous-time problems by using the Pontryagin's maximum principle. However, addressing a continuous-time optimal model by this principle considers the defined objective and constraints to be continuously differentiable. The frequency can be identified as discrete and this will cause the optimal frequency control in this study to be continuous, but not differentiable.

Additionally, as a result of the complexity of a numerical approach used by several constraints, a numerical method is used as an alternative. The main contribution of this paper can be described as follows:

1) The renewable energy sources integration into the grid with the formulation of optimal control of the battery to manage the load in each area. The model performs better with a simplified algorithm.
2) The power from renewable energy source's lower boundary and upper boundary isselected by the dynamic of the battery.
3) The frequency deviation is handled by the battery dynamic.
4) The battery is modelled as a control tool which can inject energy at any time of the control horizon to balance the network.
5) The frequency deviation is controlled by the battery during the operation.

2. Problem description

The combination of the two areas connected by the tie-line power system design provides a variety of benefits, such as improved reliability in supply, voltage control and frequency control. As presented in Fig. 1, the model aims to export and import a scheduled amount of power through a tie-line. The continuity model in Fig. 1 shows that each area presented in this study will absorb its load changes during normal operation. Area 1 (microgrid 1) is represented by a conventional source and the load, whereas area 2 (microgrid 2) is supplied by a renewable energy source, which is a combination of a photovoltaic system, a wind generator and the storage system. The total power flow into the two areas, taking into consideration the tie-line deviation ΔP_{tie} , is expressed as:

$$P_3(t) = \left(P_1(t) - P_2(t)\right) + \left(P_4(t) + P_B(t) - P_5(t)\right) \quad (1)$$

Where $P_3(t)$ is the state variable, which represents the energy flow between the tie-line, the $P_3(t)$ has its negative

and the positive value, which respond to the area frequency response characteristic. With $P_B = P_6$ or -P_7 .

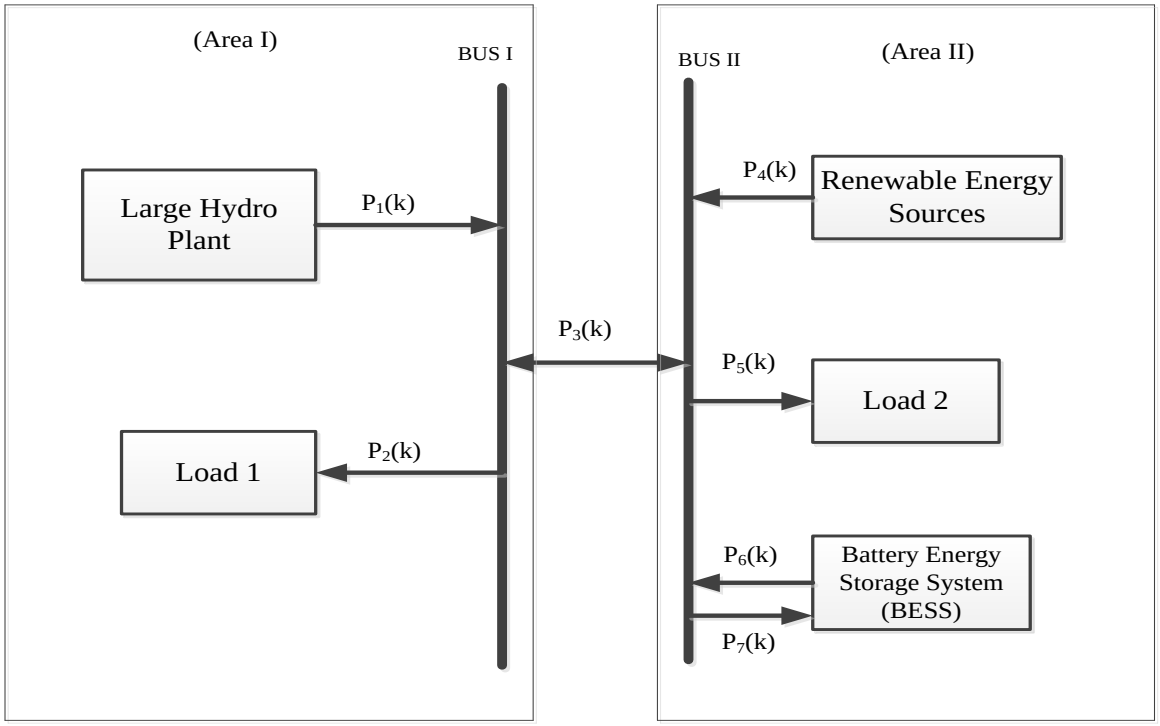

Fig. 1 Network Model

From Figure 1, $P_1(t)$ active power from the large hydro-power plant; $P_2(t)$ load demand area 1; $P_3(t)$ active power flow in the tie-line; $P_4(t)$ active power from renewable energy sources; $P_5(t)$ load demand area 2; $P_6(t)$ active power from the energy storage system; $P_7(t)$ active power that charges the energy storage system

To ensure balanced operation and maintain stability in the process in different areas, the total energy flow from various power sources must be controlled to maintain balance and meet the total energy demand of the connected load.

The total energy flow generated (EFG) by the two-area system is represented in Eq. 2.

$$EFG = P_1(t) + P_4(t) + P_6(t) \tag{2}$$

The Kirchhoff law application applied as the difference between the energy flow from the demand (END) side and the energy flow generated by the different sources is presented in Eq. 3.

$$\Delta E_e = EFG - END \tag{3}$$

where ΔE_e is the energy flow deviation.

The energy flow from the tie-line $P_3(t)$ depends on the area frequency because the hydropower plant supplies area 1 in the model. The change in the reference power setting of its own turbine-governor operating under load frequency control is proportional to the integral of the area control error (ACE). In the integration of the setting power reference, the value of k is included as a constant value that is represented as an integrator gain to the specific model, which can be derived to determine the frequency (*F*) by applying equation 4.

$$F = \frac{\Delta E_e}{\Delta(2\pi k)} \tag{4}$$

With the two areas interconnected, Eq.3 will be reduced to two by Eqs. (5) and (6).

$$\Delta E_{e1} = P_1(t) - P_2(t) \tag{5}$$

$$\Delta E_{e2} = P_4(t) + P_6(t) - P_5(t) \tag{6}$$

3. Optimisation technique

The necessary condition to optimise a model can be summarised by five control variables and one state variable, which is the energy flow between the tie. This occurs when the load change has occurred in any area. A new configuration can be achieved only when the energy flow reaches a constant value. This happens when all reference power settings are zero, which in turn occurs when the ACE is zero in every area.

3.1. *Frequency regulation*

The secondary reserves are operated until they are entirely replaced by tertiary reserves, which can be represented by Eq. 7:

$$f^{\min} \le f(t) \le f^{\max} \tag{7}$$

Where $f^{\min}$ and $f^{\max}$ are the minimum and maximum expected instantaneous frequency after a reference incident with predefined system conditions.

Figure 2 represents two microgrids interconnected via one tie-line. Tie-lines exchange power between control areas to provide inter-area support in abnormal conditions. Based on Fig. 2, the following parameters are defined: the tie-line power deviation (ΔP_{TL}), the synchronising power coefficient (P_S), $\Delta\omega_1$ and $\Delta\omega_2$ are frequency deviations in areas 1 and 2. The tie-line deviation is calculated using the following equation:

$$\Delta P_{TL} = P_S\left(\int \Delta\omega_1 dt - \int \Delta\omega_2 dt\right) \tag{8}$$

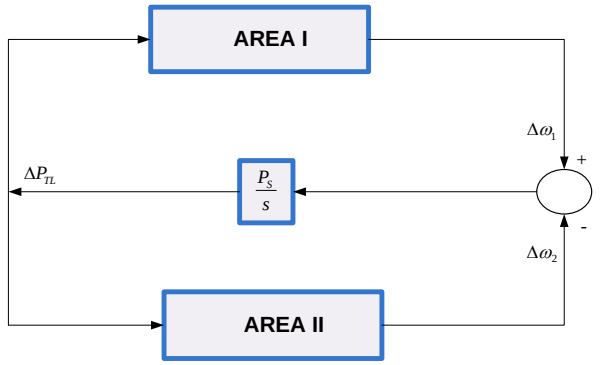

Fig. 2 Modelling of one tie-line connection [11]

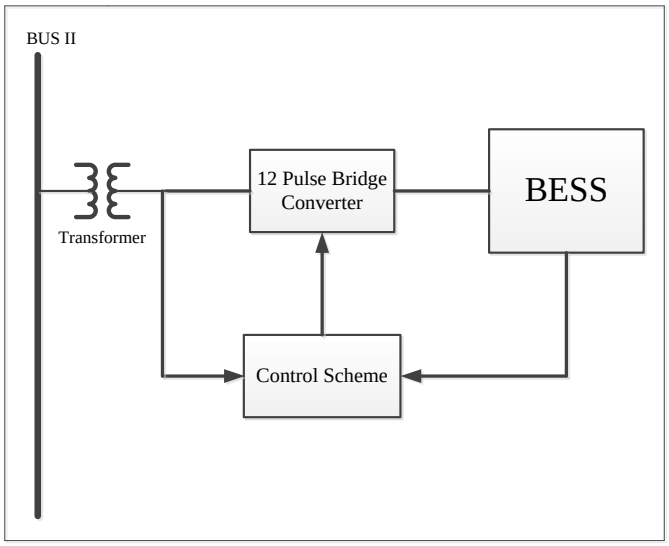

Fig. 3 Description of BESS plant

Figure 3 represents a layout diagram of the BESS plant. The main components of the BESS are the equivalent battery, composed of parallel/series connected battery cells, a 12-pulse cascaded bridge circuit connected to a Y/Δ−Y transformer and an optimal control scheme. The ideal no-load maximum D.C. voltage of the 12-pulse converter is expressed as E_{do}, as given in Eq. 9.

$$E_{d0} = E_{d01} + E_{d02} = \frac{6\sqrt{6}}{\pi} E_t \tag{9}$$

where E_t is the line to neutral r.m.s voltage, the configuration of the battery equivalent circuit is made by the battery equivalent circuit (E_{boc}), the battery overvoltage (E_{b0}), connecting and stand internal resistor (r_{bc}), (r_{ic}). Where Eq. 10 expresses D.C. current flowing into the battery

$$I_{Bdc} = \left(\frac{E_{bes} - E_{b0} - E_{boc}}{r_{bc} + r_{ic}}\right) \tag{10}$$

The energy flow from the bus to the battery (p_7) and its reactive component is determined by equations (11) and (12) respectively, taking into consideration the converter circuit analysis.

$$P_7(k) = \frac{3\sqrt{6}}{\pi} E_t I_{bess}\left(\cos\alpha_1^0 - \cos\alpha_2^0\right) \tag{11}$$

$$Q_7(k) = \frac{3\sqrt{6}}{\pi} E_t I_{bess}\left(\sin\alpha_1^0 - \sin\alpha_2^0\right) \tag{12}$$

where α_1^0 and α_2^0 are the firing delay angle of converter 1 and converter 2 used in the BESS model.

3.2. *Objective function*

In the design model of the power system of the interconnected area, the area agrees on the exportation or importation of a scheduled amount of energy flow through tie-lines. The aim is to ensure each area absorbs its load changes during normal operation. The LFC is implemented in one area, which is the renewable energy source. This is achieved by maintaining the net power tie-line power flow out of each area at its scheduled value.
The objective function is a way of minimising the ACE.

$$ACE_i = \sum_{j=1}^{t} \Delta P_{ij} + B_i \Delta\omega_i \tag{13}$$

In this model, to optimise Eq. 13, fmincon, a function included in MatLab's optimisation toolbox, is used, taking into consideration the non-linearity of the system. Eq. 6 makes a canonical form, which is represented by Eq. 14:

$$Min\ f(x) \tag{14}$$

Thus, Eq. 14 is subjected to the following constraints:

$$\begin{cases} A.X \le b\ (linear\ inequality\ constra\,\text{int}) \\ A_{eq}.X = b_{eq}\ (linear\ equality\ constra\,\text{int}) \\ L_B \le X \le U_B\ (lower\ and\ upper\ bounds) \end{cases} \tag{15}$$

3.3. System constraints

To identify the constraints applied in the model, Eq. 15 will be derived in a matrix format to achieve the form presented by Eq. 16.

$$A_{eq} = \begin{bmatrix} 1 & 0 & -1 & 0 & 1 & 0 & -1 & 0 & 1 & 0 & -1 & 0 \\ 0 & -1 & 0 & 1 & 0 & -1 & 0 & 1 & 0 & -1 & 0 & 1 \end{bmatrix} \quad (16)$$

Where X is taken as a vector in the model made from Eq. 17.

$$b_{eq} = \begin{bmatrix} P_1(t) \\ P_2(t) \end{bmatrix} \quad (17)$$

3.4. Dynamics of battery state of charge

The battery is discharged to cover the deficit. It can be expressed by an equation for the SOC, which is:

$$SOC(t+1) = SOC(t) - \frac{\Delta t_n}{E_{nominal}} \sum_{i=1}^{t} P_6(t) \quad (18)$$

where SOC is the state of charge of the battery; $P_6(t)$ is the power flow from the battery (discharge), $E_{nominal}$ Nominal Energy, n is the battery efficiency.

Where the storage system is taken as the vital parameter to the model, the dynamic of the storage system must not be less than the minimum allowable capacity and must not be more than the maximum permissible size as expressed by Eq. 19:

$$SOC^{min} \leq SOC(t) \leq SOC^{max} \quad (19)$$

Equation 19 and 20 can be presented under a matrix format expressed by the battery dynamic to model the inequality constraint matrix given by Eqs. 20 and 21

$$A_{ineq} = \begin{bmatrix} 0 & 0 & 0 & 0 & 0 & 0 & 0 & 0 & 0 & 0 & k & 0 \\ 0 & 0 & 0 & 0 & 0 & 0 & 0 & 0 & 0 & 0 & k & k \\ 0 & 0 & 0 & 0 & 0 & 0 & 0 & 0 & 0 & 0 & -k & 0 \\ 0 & 0 & 0 & 0 & 0 & 0 & 0 & 0 & 0 & 0 & -k & -k \end{bmatrix} \quad (21)$$

$$b_{ineq} = \begin{bmatrix} soc^{\max} - soc(0) \\ soc^{\max} - soc(0) \\ soc(0) - soc^{\min} \\ soc(0) - soc^{\min} \end{bmatrix} \quad (22)$$

The control horizon has a period of 24 hours, where the optimal control is represented by the vector X which contains the energy flow for the sampling intervals. There are linear inequality constraints of which two Eqs. 21 and 22 are derived from Eq. 15. When the optimal configuration is achieved, the corresponding energy flow control at each sampling interval is repeatedly obtained by solving the Eq. 15, with its lower and upper boundary constraints.

3.5. Power flow limitations

For equipment safety purposes, all power flows should be kept within the minimum and maximum limits according to the design specifications given by the manufacturer. These boundary constraints are expressed as described in Eqs. 23, 24 and 25.

Equation 23 takes into consideration the law of supply and demand and ensures that power is supplied by the renewable energy sources, the conventional power source and the discharge of the battery.

$$P_1(t) \geq 0;\ P_5(t) \geq 0;\ P_6(t) \geq 0; \quad (23)$$

Each energy source is constrained by minimum and maximum values as specified in equation (23):

$$P_i^{\min}(t) \leq P_i(t) \leq P_i^{\max}(t) \quad (24)$$

The tie-line constraint is represented by Eq. 25 to ensure that each area maintains the net energy flow out of the area at its scheduled value, in order for the area to absorb its own load changes.

$$P_3^{\min}(t) \leq P_3^{\max}(t) \quad (25)$$

3.6. Power balance

By neglecting all converter power losses, the power balance constraints to be satisfied at different nodes of the system, are expressed in Eq. 26.

The total power flowing along the tie-line is defined as a constraint, which will be:

$$P_1(t) - P_2(t) \pm P_3(t) + P_4(t) - P_5(t) + P_6(t) \quad (26)$$

Where $P_3(t)$ is defined as a state variable representing the dynamic of the energy flow between the two areas.

Based on the proposed flowchart depicted in Fig. 4, the main steps of the BESS control strategy can be described as follows:

1) Parameters initialisation;
2) Equalities and inequalities constraints checking;
3) Solving and minimisation of the objective function;
4) Applying optimal control input;
5) Evaluations of load area changes;
6) Active power injection or power drawn;
7) End process.

4. Simulation results and analysis

Table 1 describes the real value of the designed model system parameters. These values will be used to test and validate the proposed model. The system of two interconnected networks as described in Fig. 1 with the battery energy storage system in area II is simulated through Matlab Software. Thus, it is important to note that the incremental model of the battery storage system is effected and incorporated into a single area system and an interconnected two area power system, where the control of the model is given to the dynamic of battery energy storage. The optimal control solution is used to optimise the deviation of the frequency between areas and the battery to compensate for the energy needed to obtain the frequency deviation and

tie line power errors close to zero while ensuring a balance minimisation between the energy generation and the load demand.

For better performance of the energy flow on the network, the battery energy storage system will operate in discharging mode during the load deviation period to fill any gap created when any of the areas pick up or lose the load and will switch to charging mode when the system is stable. Therefore, only the discharging mode behaviour of battery energy storage is examined on LFC.

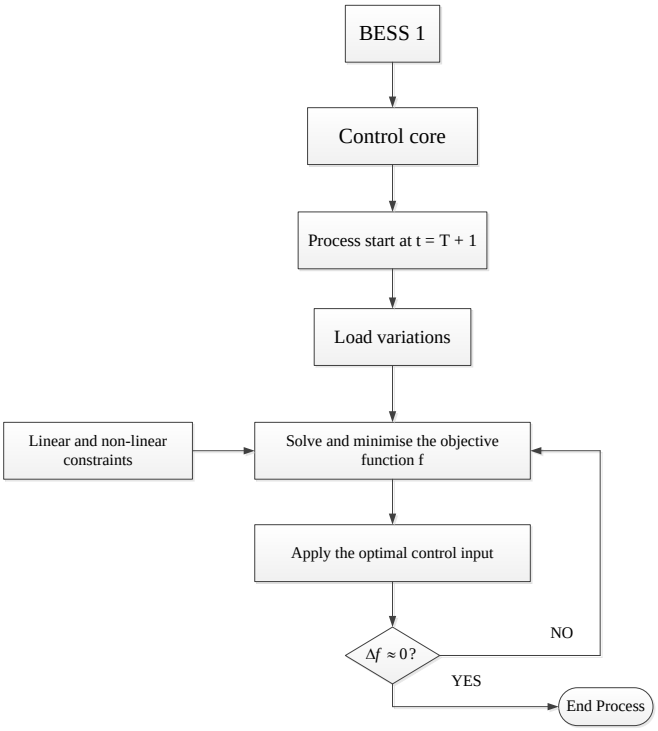

Fig. 4 Proposed flowchart of BESS control

From Fig. 5 to Fig. 14, as well as Table 2 it can be observed that the application of the optimal battery control causes considerable deviation of the frequency and power tie and also reduces settling time. Therefore, when the optimal control of the battery is applied, the steady-state value of the time error is reduced. From Figs.10 and 11 the load frequency oscillation settles around 0.2 for the two-system area. This is a better model performance compared to the conventional controllers such as PID or PI, whose average was close to 12 seconds.

Table 1 Power system used data [28]

Parameters	Value
F	60 Hz
$P_{r1} = P_{r2}$	1000 MW
$K_{p1} = K_{p2}$	120 Hz/p.u
$T_{P1=}T_{P2}$	20.0S
$K_{r1} = K_{r2}$	0.5
$T_{r1=}T_{r2}$	10.0 S
$T_{g1} = T_{g2}$	0.08 S
$T_{t1} = T_{t2}$	0.3
R_1	2.4 Hz/p.u MW
$B_1 = B_2$	0.425
BES	10 MW – 40 MWh

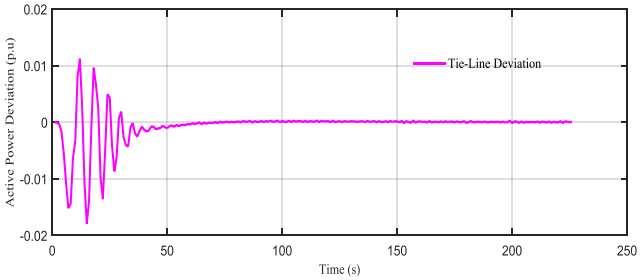

Fig. 5 Responses of power system with BES for 2% step load increase in area I.

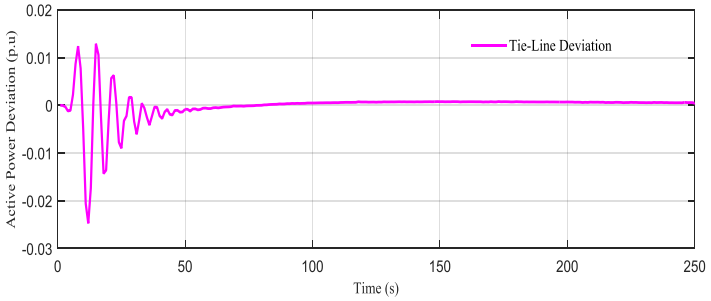

Fig. 6 Responses of power system with BES for 2% step load increase in area II.

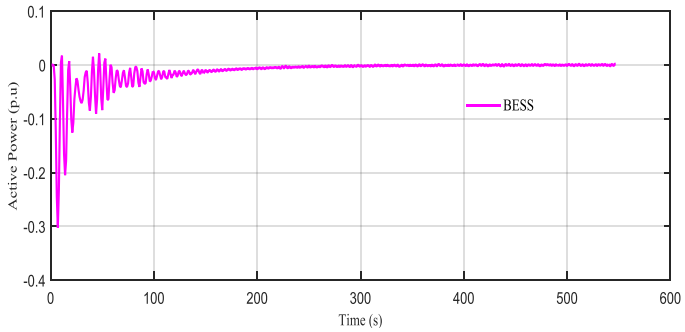

Fig. 7 BES under discharging mode (not control when the load increases in area I).

Additionally, Table 2 gives the system characteristics of the interconnected model with and without battery energy storage. This compared the results of the proposed model with some research studies [27], [25], [24]. The system parameters considered are frequency deviations in area I and II and the power line interconnecting those two areas. To show the effectiveness of the proposed model, the comparison was based on two cases; the first case gives the settling time without the use of the battery. The second case was based on the comparison of the settling time with the use of the battery. As observed, the peak deviation has strong amplitude in many cases when the battery is not taken into account. Considering the deviation of frequency in area I, we have, from $-0.102Hz$ to $-0.024Hz$ giving the frequency difference between two areas in the proposed model, while for reference [27] we have $-0.12404Hz$ to $-0.0317Hz$; and for [24] $0.01Hz$ to $0.02Hz$. The analysis of Table 2 reveals the effectiveness of the use of the power flow from BES in the control system of the proposed model. The frequency responses from areas I and II are good based on the model presented in Eq. 27.

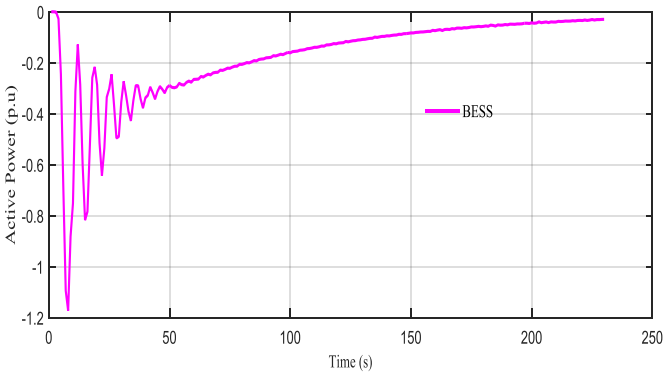

Fig. 8 BES control under discharging mode (when the load increases in area I)

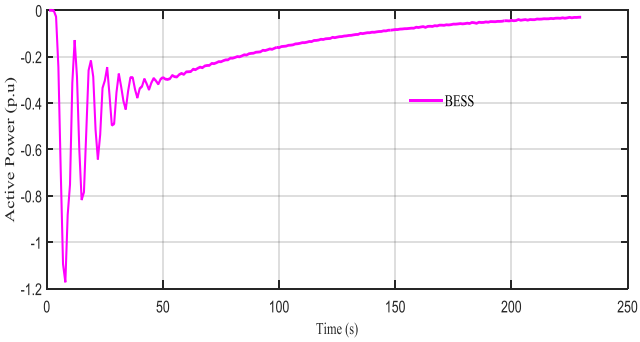

Fig. 9 BES control under discharging mode (when the load increases in area II)

Table 2 Peak deviations, frequency deviations, power tie deviation with and without BES system

References	Parameters	Peak deviation without BES	Settling Time	Peak deviation with BES	Settling Time
This Paper	$\Delta F_1(H_Z)$	-0.102	130	-0.024	50
	$\Delta F_2(H_Z)$	-0.122	130	-0.022	50
	$\Delta P_{tie}(MW)$	-0.008	130	-0.003	50
Paper [25]	$\Delta F_1(H_Z)$	0.02	41.44	0.02	13.59
	$\Delta F_2(H_Z)$	0.03	40.32	0.02	27.81
	$\Delta P_{tie}(MW)$	--	--	--	--
Paper [27]	$\Delta F_1(H_Z)$	-0.12404	150	-0.03176	50
	$\Delta F_2(H_Z)$	-0.12219	150	-0.02894	50
	$\Delta P_{tie}(MW)$	-0.00969	150	-0.00528	50
Paper [24]	$\Delta F_1(H_Z)$	0.01	42.48	0.02	--
	$\Delta F_2(H_Z)$	--	--	--	--
	$\Delta P_{tie}(MW)$	4.77	34.56	0.01	--

Eq. 27 determines the improvement from the control model when the battery is applied, based on the values given in Table 2.

$$CI = \left(\frac{CBN - CWB}{CBN} \right) \times 100\% \tag{27}$$

where: CI is a control improvement, CBN when battery has not been applied in the model, and CWB when the battery has been included in the model.

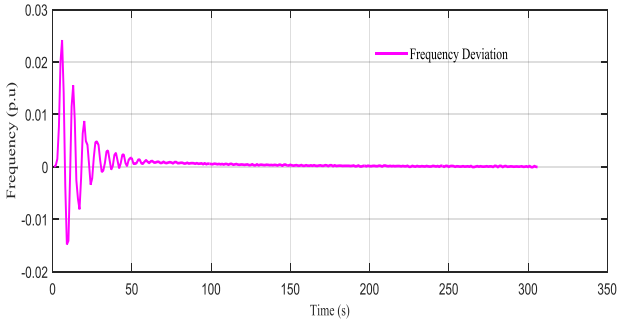

Fig. 10 Responses of the frequency deviation with BES for 2% step load increase in area I

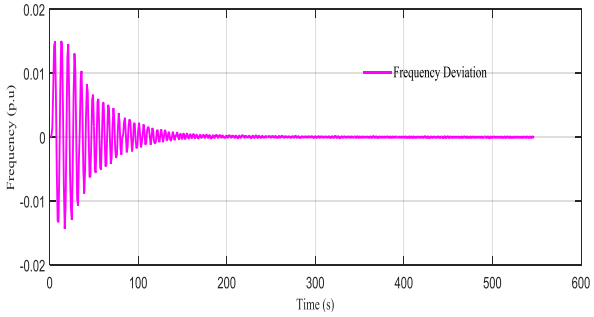

Fig.11 Responses of the frequency deviation without BES for 2% step load increase in area I

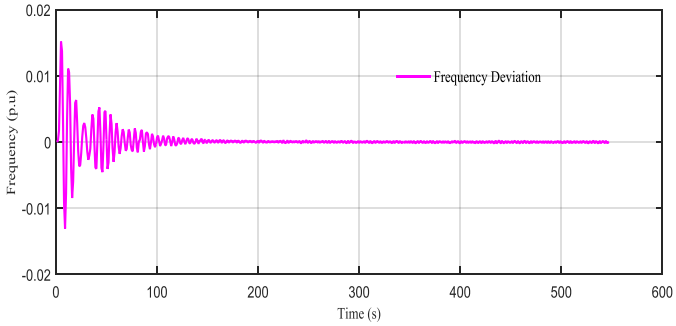

Fig.12 Responses of power system without BES for 2% step load increase in area II

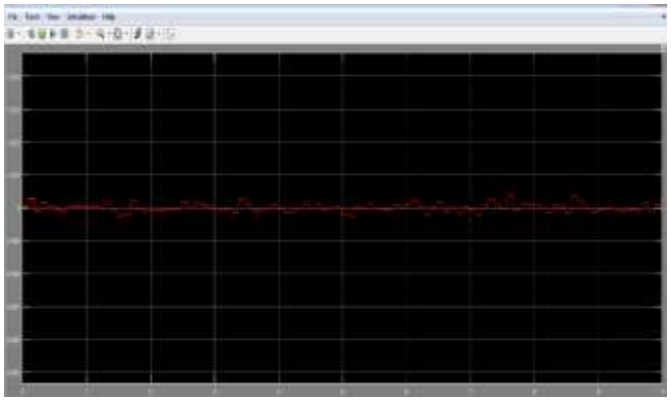

Fig. 13 Load variation in area I

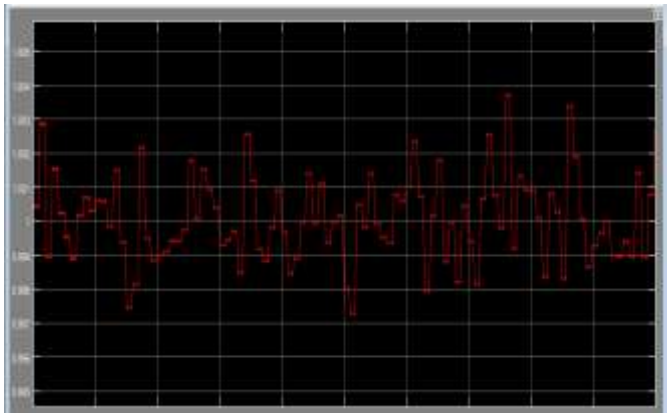

Fig. 14 Load variation in area II

5. Conclusion

The load frequency control is an essential factor in the renewable energy environment, especially for the power fluctuation due to renewable energy sources. In this paper, load frequency control is employed in only one area, where renewable energy is applied as the source. Control is achieved by the optimisation of the output power of the energy storage system, which acts as the state variable of the model. The frequency deviation and the power line profile demonstrated the robustness of the model. The scenarios to analyse the response of the two areas under load variations have also been taken into consideration with and without considering the BES system. It is also observed that the use of the BES system has an advantage compared to the system where the BES is not applied. The development of the mathematical model for the battery dynamic to determine the new control strategy has shown that regulating the ACE to zero is suitable for load frequency control in a multi-micro grid system. The simulation results show that the proposed design strategy can enhance the frequency deviation with significant value of about 80% of control improvement.

References

[1] D. H. T. R. C. Bansal and M. W. S. N. T. Mbungu, “Predictive Active Power Control of Two Interconnected Microgrids,” pp. 1–15, 2018.

[2] R. Umrao and D. K. Chaturvedi, “Load Frequency Control Using Polar Fuzzy Controller,” 2010.

[3] A. Stefanov, C.-C. Liu, M. Sforna, M. Eremia, and R. Balaurescu, “Decision support for restoration of interconnected power systems using tie lines,” *IET Gener. Transm. Distrib.*, vol. 9, no. 11, pp. 1006–1018, 2015.

[4] N. T. Mbungu, R. C. Bansal, R. Naidoo, V. Miranda, and M. Bipath, “An optimal energy management system for a commercial building with renewable energy generation under real-time electricity prices,” *Sustain. Cities Soc.*, vol. 41, 2018.

[5] R. T. Mukwanga W. Siti, “No Title,” *Optim. Energy Control a Grid Connect. Sol. Wind Based Electr. Power Plant Appl. Time Use Tarif.*, vol. 10, no. 2, 2015.

[6] N. T. Mbungu, R. Naidoo, R. C. Bansal, and M. Bipath, “Optimal single phase smart meter design,” *J. Eng.*, vol. 2017, no. 13, pp. 1220–1224, 2017.

[7] K. H. Solangi, M. R. Islam, R. Saidur, N. A. Rahim, and H. Fayaz, “A review on global solar energy policy,” *Renew. Sustain. Energy Rev.*, vol. 15, no. 4, pp. 2149–2163, 2011.

[8] N. T. Mbungu, R. C. Bansal, and R. Naidoo, “Smart Energy Coordination of a Hybrid Wind / PV with Battery Storage Connected to the Grid,” in *IET Renewable Power Generation*

Conference, 2018, pp. 1–6.
[9] Y. Levron, J. M. Guerrero, and Y. Beck, "Optimal Power Flow in Microgrids With Energy Storage," *Power Syst. IEEE Trans.*, vol. PP, no. 99, pp. 1–9, 2013.
[10] A. F. Zobaa and R. C. Bansal, *HANDBOOK OF RENEWABLE ENERGY TECHNOLOGY*, Singapore: 2011.
[11] D. H. Tungadio, R. C. Bansal, and M. W. Siti, "Optimal Control of Active Power of Two Micro-grids Interconnected with Two AC Tie-Lines," *Electr. Power Components Syst.*, vol. 45, no. 19, pp. 2188–2199, 2017.
[12] A. Hasib Chowdhury and M. Asaduz-Zaman, "Load Frequency Control of Multi-Microgrid Using Energy Storage System," *8th Int. Conf. Electr. Comput. Eng.*, no. October, pp. 548–551, 2014.
[13] H. S. Lee, B. G. Koo, S. W. Lee, W. Kim, and J. H. Park, "Optimal control of BESS in microgrid for islanded operation using fuzzy logic," *Proc. - Int. Conf. Intell. Syst. Model. Simulation, ISMS*, vol. 2015–Septe, pp. 468–473, 2015.
[14] M. Martiskainen and J. Coburn, "The role of information and communication technologies (ICTs) in household energy consumption-prospects for the UK," *Energy Effic.*, vol. 4, no. 2, pp. 209–221, 2011.
[15] W. Zhou, C. Lou, Z. Li, L. Lu, and H. Yang, "Current status of research on optimum sizing of stand-alone hybrid solar-wind power generation systems," *Appl. Energy*, vol. 87, no. 2, pp. 380–389, 2010.
[16] T. Ma, H. Yang, L. Lu, and J. Peng, "Optimal design of an autonomous solar-wind-pumped storage power supply system," *Appl. Energy*, vol. 160, pp. 728–736, 2015.
[17] M. Herrando and C. N. Markides, "Hybrid PV and solar-thermal systems for domestic heat and power provision in the UK: Techno-economic considerations," *Appl. Energy*, vol. 161, pp. 512–532, 2016.
[18] N. T. Mbungu, R. Naidoo, R. C. Bansal, and M. Bipath, "Optimisation of grid connected hybrid photovoltaic-wind-battery system using model predictive control design," *IET Renew. Power Gener.*, vol. 11, no. 14, 2017.
[19] M. Vahedipour, A. Anvari-Moghaddam, and J. Guerrero, "Evaluation of Reliability in Risk-Constrained Scheduling of Autonomous Microgrids with Demand Response and Renewable Resources," *IET Renew. Power Gener.*, vol. 12, pp. 657–667, 2018.
[20] M. Martínez, M. G. Molina, and P. E. Mercado, "Optimal sizing method of vanadium redox flow battery to provide load frequency control in power systems with intermittent renewable generation," *IET Renew. Power Gener.*, vol. 11, no. 14, pp. 1804–1811, 2017.
[21] M. W. Siti, D. V. Nicolae, A. A. Jimoh, and A. Ukil, "Reconfiguration and load balancing in the LV and MV distribution networks for optimal performance," *IEEE Trans. Power Deliv.*, vol. 22, no. 4, pp. 2534–2540, 2007.
[22] V. S. Sundaram and T. Jayabarathi, "Load Frequency Control using PID tuned ANN controller in power system," *2011 1st Int. Conf. Electr. Energy Syst. ICEES 2011*, pp. 269–274, 2011.
[23] J. Ranjan, B. Shaw, and B. Kumar, "Engineering Science and Technology , an International Journal Application of adaptive-SOS (ASOS) algorithm based interval type-2 fuzzy-PID controller with derivative filter for automatic generation control of an interconnected power system," *Eng. Sci. Technol. an Int. J.*, vol. 21, no. 3, pp. 465–485, 2018.
[24] M. Nandi, C. K. Shiva, and V. Mukherjee, "Frequency stabilization of multi-area multi-source interconnected power system using TCSC and SMES mechanism," *J. Energy Storage*, vol. 14, pp. 348–362, 2017.
[25] N. Gupta and N. Kumar, "Particle Swarm Optimization based Automatic Generation Control of Interconnected Power System incorporating Battery Energy Storage System," *Procedia Comput. Sci.*, vol. 132, pp. 1562–1569, 2018.
[26] B. Ogbonna and S. N. Ndubisi, "Neural Network Based Load Frequency Control for Restructuring Power Industry," vol. 31, no. 1, pp. 40–47, 2012.
[27] S. . Aditya and D. Das, "Battery energy storage for load frequency control of an interconnected power system," *Electr. Power Syst. Res.*, vol. 58, no. 3, pp. 179–185, 2001.
[28] S. Kalyani, S. Nagalakshmi, and M. R, "Load Frequency Control Using Battery Energy Storage System in Interconnected Power System," *Comput. Commun. Netw. Technol. (ICCCNT), 2012 Third Int. Conf.*, no. July, 2012.